Published in final edited form as:
Plast Reconstr Surg. 2012 June ; 129(6): 1247–1257. doi:10.1097/PRS.0b013e31824ec3dc.

AN INJECTABLE ADIPOSE MATRIX FOR SOFT TISSUE RECONSTRUCTION

Iwen Wu, B.S.[1,*], **Zayna Nahas, M.D.**[2,*], **Kelly A. Kimmerling, B.S.**[1], **Gedge D. Rosson, M.D.**[3], and **Jennifer H. Elisseeff, Ph.D.**[1]

[1]Department of Biomedical Engineering, Johns Hopkins University School of Medicine, Baltimore, MD

[2]Department of Otolaryngology, Johns Hopkins University School of Medicine, Baltimore, MD

[3]Department of Plastic Surgery, Johns Hopkins University School of Medicine, Baltimore, MD

Abstract

Background—Soft tissue repair is currently limited by the availability of autologous tissue sources and the absence of an ideal soft tissue replacement comparable to native adipose tissue. Extracellular matrix (ECM)-based biomaterials have demonstrated great potential as instructive scaffolds for regenerative medicine, mechanically and biochemically defined by the tissue of origin. As such, the distinctive high lipid content of adipose tissue requires unique processing conditions to generate a biocompatible scaffold for soft tissue repair.

Methods—Human adipose tissue was decellularized to obtain a matrix devoid of lipids and cells, while preserving ECM architecture and bioactivity. To control degradation and volume persistence, the scaffold was crosslinked using hexamethylene diisocyanate and 1-Ethyl-3-(-3-dimethylaminopropyl) carbodiimide. In vitro studies with human adipose-derived stem cells were used to assess cell viability and adipogenic differentiation on the biomaterial. In vivo biocompatibility and volume persistence were evaluated by subcutaneous implantation over 12 weeks in a small animal model.

Results—The scaffold provided a biocompatible matrix supporting the growth and differentiation of adipose-derived stem cells in vitro. Crosslinking the matrix increased its resistance to enzymatic degradation. Subcutaneous implantation of the acellular adipose matrix in Sprague-Dawley rats showed minimal inflammatory reaction. Adipose tissue development and vascularization was observed in the implant, with host cells migrating into the matrix indicating the instructive potential of the matrix for guiding tissue remodeling and regeneration.

Conclusions—With its unique biological and mechanical properties, decellularized adipose ECM is a promising biomaterial scaffold that can potentially be used allogenically for the correction of soft tissue defects.

Introduction

There is a significant need for soft tissue replacements in the field of reconstructive surgery. Autologous tissue is currently the treatment of choice for repairing soft tissue defects due to trauma, tumor resection, and congenital defects.1-3 However, current autologous fat transfer techniques have a number of limitations. For many HIV patients suffering from lipodystrophy and patients undergoing chemotherapy for cancer, the associated cachexia leaves them without the adipose volume required for autologous tissue transfer. Additionally, the persistence of fat transfer varies widely and is often surgeon, technique, and patient dependent. With resorption causing up to 40-55% reduction of total graft volume over 6 months, multiple procedures are often required in order to maintain the desired

Commercial associations or financial disclosures

Iwen Wu- Author is an inventor on IP licensed to Aegeria Soft Tissue LLC

Zayna Nahas- Author is an inventor on IP licensed to Aegeria Soft Tissue LLC

Kelly A. Kimmerling- no commercial associations or financial disclosures

Gedge D. Rosson- Author is an inventor on IP licensed to Aegeria Soft Tissue LLC

Jennifer H. Elisseeff- Author is an inventor on IP licensed to Aegeria Soft Tissue LLC

correction and volume limitations need to be taken into account to prevent necrosis.4

Supplier	Products
Sigma	Peracetic acid
	Triton X-100
	EDTA
	$MgCl_2$
	HCl
	p-dimethylaminobenzaldehyde
	Chloramine T-hydrate
	Formaldehyde
	Glutaraldehyde
	Ethanol
	Xylene
	N'-(3-dimethylaminopropyl)-N-ethylcabordiimide N-hydroxysuccinimide
	2-(N-morpholino)ethanesulfonic acid
	Na_2HPO_4
	Isopropanol
	NaCl
	Tris-HCl
	Hematoxylin
	Eosin
	Masson's trichrome kit
	Dexamethasone
	Indomethacin
	Methylisobutylxanthine
	Insulin
	Triethyl phosphate
Gibco	DMEM F-12
	High Glucose DMEM
	PBS
	Penicillin/Streptomycin
Thermo Scientific	Hyclone Defined FBS
Worthington	Collagenase I
	Papain
Roche	DNase
Invitrogen	Hoechst
	LIVE/DEAD cytotoxicity kit
	Alexafluor 546 goat anti-mouse IgG2a
	Alexafluor 488 goat anti-mouse IgG1
Fitzgerald	Rabbit anti-collagen I
Abcam	Mouse anti-CD31
BD Pharmingen	Anti-rat CD44, Mouse IgG2a
Jackson	FITC goat anti-rabbit IgG
Vector Labs	Vectashield with DAPI

Author Disclosure Statement

Authors are inventors on IP licensed to Aegeria Soft Tissue LLC.

Finally, implanted adipose tissue can lead to post-operative calcifications which is detrimental for patients with a history of breast cancer as this may interfere with early radiologic detection of cancer.5

Developments in plastic surgery and microsurgical techniques have established autologous tissue flaps as excellent options for post-mastectomy breast reconstruction, offering patients outstanding aesthetic outcomes without the concern for long-term alloplastic implant complications such as capsular contracture and rupture.2, 6 However, a complex procedure like autologous flap transplantation carries its own set of risks including necrosis of transplanted tissue7 and donor site morbidity, such as abdominal wall weakness, scarring, and hernia.2, 8-10 Perforator flap techniques and new imaging protocols have been developed to help leave the musculature intact in order to decrease donor site morbidity; nevertheless, they remain complex and lengthy undertakings.11-15

Regenerative medicine approaches to soft tissue reconstruction provide a potential alternative in which biomaterials facilitate tissue regeneration in the defect area, thus avoiding the need for tissue transplantation from a donor site. Several studies have investigated the use of various synthetic polymers in conjunction with a cell delivery using polyethylene glycol, poly L-lactic acid, polyglycolic acid, and poly(lactic-co-glycolic) acid copolymers.16-25 Naturally-derived polymer scaffolds such as collagen, hyaluronic acid, gelatin, silk fibroin, alginate, and fibrin have also been applied to adipose tissue engineering. 26-33 Additionally, researchers have tried to harness extracellular matrix (ECM) components for use in adipose tissue engineering using ECM derived from EHS sarcomas (Matrigel), adipose tissue, dermis, muscle, and placenta.34-44 However, a recent review highlights the lack of three-dimensional scaffolds derived from adipose tissue.45

Here we show the development of a novel adipose-derived extracellular matrix biomaterial that serves as a three-dimensional scaffold for tissue regeneration. Intact ECM-based biomaterials have not been previously studied *in vivo* for use as a volume-stable soft tissue implant that can be crosslinked to control degradation properties.45, 46 We hypothesized that intact human adipose tissue could be decellularized to obtain a matrix that would provide an instructive environment for the repair of soft tissue defects. To control the rate of degradation, chemical crosslinkers can be used to reinforce the collagen and other proteins in matrix-based scaffolds. Thus the aims of this study are to develop a biocompatible adipose-derived biomaterial by removing lipids and resident cells from adipose tissue, use crosslinkers to modulate degradation properties of the extracellular matrix, and evaluate the biocompatibility of the matrix in vivo.

Materials and Methods

Adipose extracellular matrix was produced by decellularizing adipose tissue using a combination of mechanical and chemical processing steps. Upon obtaining the acellular adipose tissue, the material was characterized, followed by crosslinking to modulate degradation profiles. In vitro and in vivo biocompatibility studies were performed to investigate the cell and tissue response to the adipose-derived biomaterial. Materials were obtained from Sigma-Aldrich (St. Louis, MO) unless otherwise noted.

Adipose-derived stem cell isolation

Subcutaneous adipose tissue was obtained from patients (n=3) undergoing abdominoplasty procedures with approval from Johns Hopkins Medicine Institutional Review Board. Adipose-derived stem cells (ASCs) were isolated by digestion with 1 mg/mL collagenase I (Worthington, Lakewood, NJ) in DMEM F-12 (Gibco, Grand Island, NY) for 1.5 hours on an orbital shaker at 37∞C. The resulting cell suspension was centrifuged and filtered

through 70 uM and 40 uM cell strainers. ASCs were seeded at 10,000 cells/cm^2 and cultured in DMEM-F12 supplemented with 10% fetal bovine serum (Thermo Scientific HyClone, Logan, Utah).

Adipose extracellular matrix preparation

Subcutaneous adipose tissue was subjected to mechanical processing and extensive rinsing followed by incubation with 0.1%, 1%, 3%, or 5% peracetic acid for 3 hours to remove cells. Samples were brought back to physiological pH using PBS and incubated overnight with 1% Triton X-100 in 2 mM EDTA to remove residual lipids. Finally, samples were treated with 600 U/mL DNase (Roche, Indianapolis, IN) in 10 mM $MgCl_2$ overnight at 37∞C.

Material characterization

Biochemical assays—Adipose ECM scaffolds were lyophilized and digested in a 125 ug/mL papainase solution (Worthington) for 16 hours at 60∞C. DNA content was determined by fluorescence intensity using 1 ug/mL Hoechst dye (Molecular Probes, Eugene, OR) in TNE buffer.47 Total collagen content was determined by a hydroxyproline assay with acid hydrolysis in 6N hydrochloric acid at 115∞C, followed by reaction with *p*-dimetylaminobenzaldehyde and chloramine-T hydrate to obtain an absorbance reading at 525 nm.48

Scanning electron microscopy (SEM)—Samples were prepared for SEM by fixing in 3.0% formaldehyde/1.5% glutaraldehyde in 0.1 M sodium cacodylate buffer with 2.5% sucrose for 1 hour. Samples were then post-fixed with 1% osmium tetroxide for 30 minutes before dehydration with graded ethanol solutions. Samples were dried using CO_2 critical point drying followed by sputter-coating with platinum and images were taken with FEI Quanta 200 SEM (Hillsboro, OR).

Crosslinking

Crosslinking of adipose extracellular matrix—Adipose ECM was crosslinked using 1-Ethyl-3-(-3-dimethylaminopropyl) carbodiimide hydrochloride (EDC) and *N*-hydroxysuccinimide (NHS) in 50 mM 2-(*N*-morpholino) ethanesulfonic acid buffer at pH 5.5.49 Samples were incubated with crosslinking solutions for 4 hours at concentrations of 5, 10, 50, and 100 mM EDC with an EDC:NHS molar ratio of 2:1. Residual crosslinkers were removed by rinsing with 0.1M Na_2HPO_4 for 2 hours followed by four additional 30 minute incubations with distilled water.

EDC crosslinking was compared with hexamethylene diisocyanate (HMDC). Due to its instability in aqueous solutions, previous studies have used secondary alcohols as the solvent or used surfactants to preserve HMDC reactivity.50, 51 For the secondary alcohol suspension, 1% and 5% HMDC solutions were dissolved in 2-propanol and samples crosslinked for 4 hours. Alternatively, samples were crosslinked with 1% and 5% HMDC in a surfactant solution containing 1% Tween 20 in a phosphate buffer (0.054 M Na_2HPO_3, 0.013 M NaH_2PO_4) at pH 7.4 for 4 hours. Residual crosslinkers and surfactant was removed with distilled water.

Resistance to enzymatic degradation—The crosslinking conditions were characterized by comparing susceptibility to enzymatic degradation. Crosslinked samples and uncrosslinked controls (n=3) were lyophilized and incubated with 200 U/mL collagenase I in 0.05 M Tris-HCl (pH 7.5) at 37∞C.50, 52 At timepoints of 1, 3, 8, 16, and 24 hours, the samples were spun down and supernatants collected and stored at -20∞C until

completion of the experiment and fresh collagenase added to samples. At 24 hours, any remaining ECM was digested with papainase. Finally, the supernatants and papain digested samples were analyzed via the collagen assay to quantify solubilized collagen. The percentage of total collagen degraded was calculated at the different timepoints.

In vitro studies

To evaluate cell viability on the crosslinked matrices, cells were seeded on the scaffolds and cultured for 5 days in ASC maintenance media (DMEM-F12, 10% FBS, 100 U/mL penicillin, 10 ug/mL streptomycin). Cell viability was assessed using a LIVE/DEAD Viability/Cytotoxicity Kit (Invitrogen, Carlsbad, CA). Cell-ECM scaffolds were incubated with 1 uM calcein AM and 4 uM ethidium homodimer-1 in DMEM-F12 for 30 minutes at 37∞C to visualize live and dead cells.

Adipogenic differentiation was carried out for ASCs seeded in the matrix and supplemented with adipogenic induction media (1 μM dexamethasone, 200 μM indomethacin, 500 μM methylisobutylxanthine, 10 μg/ml insulin, 1% penicillin/streptomycin, and 10% FBS in High Glucose DMEM). Cells were differentiated for 7 days in culture on an orbital shaker and fixed for histological analysis.

In vivo biocompatibility

Biocompatibility was evaluated in an in vivo rat study with approval from the Johns Hopkins Animal Care and Use Committee. A total of 18 subcutaneous injections (6 per crosslinking condition) were carried out in two male and two female Sprague-Dawley rats (n=4) between 4-13 weeks old. The following conditions were used: uncrosslinked control, 5 mM EDC-crosslinked, and 1% HMDC-crosslinked in Tween 20, with 300 ul injections of each condition along the dorsum. Implants were removed after 2 and 3 weeks and fixed for histology.

Upon completion of the initial study, a longer term study was carried out with 6-week old female Sprague Dawley rats (n=12) over the course of 12 weeks. Animals were grouped by study endpoints of 1, 4, and 12 weeks. Uncrosslinked adipose-derived matrix was injected subcutaneously to characterize the immune response and tissue remodeling without introducing additional crosslinkers which can potentially induce a different inflammatory response.

Histology—Specimens for paraffin embedding were fixed with 10% formalin, dehydrated through graded ethanol solutions, cleared in xylene, and embedded in paraffin. Samples were sectioned at 5 um thickness and stained with hematoxylin and eosin or Masson’s trichrome. For Oil Red O (0.75% (w/v) in 36% triethyl phosphate) staining of lipids, samples were fixed and infiltrated with graded sucrose solutions, followed by OCT embedding and cryosectioned in order to visualize new adipose tissue formation.

For immunostaining, antigen retrieval was carried out with Tris-EDTA pH 9.0 buffer at 100∞C for 30 minutes. Slides were incubated with primary antibodies for collagen I (Fitzgerald, Acton, MA), CD31 (Abcam, Cambridge, MA), and CD44 (BD Pharmingen, San Diego, CA) overnight, followed by incubation with secondaries: FITC goat anti-rabbit IgG (Jackson), Alexafluor 546 goat anti-mouse IgG2a and Alexafluor 488 goat anti-mouse IgG1 (Invitrogen) for two hours and coverslipped with Vectashield with DAPI (Vector Labs, Burlingame, CA).

Results

Adipose extracellular matrix

We obtained an acellular adipose-derived matrix that retains properties from adipose tissue for soft tissue repair. The processing methods developed for decellularizing adipose tissue resulted in significant macroscopic changes as lipids and other cell components were removed. Intracellular lipids contribute to the characteristic yellow color of intact adipose tissue and as the lipids are removed, the ECM remains as a white fibrous tissue scaffold (Fig. 1). Histological analysis revealed the complete removal of nuclei and the absence of intracellular lipid vacuoles characteristic of adipose tissue. Immunostaining for collagen I confirms it as the predominant component of adipose ECM.

Material characterization

Various processing conditions were compared to determine the optimal processing scheme to decellularize adipose tissue. Biochemical analysis of the composition of adipose scaffolds showed little donor variability across the three different donors. Samples treated with 0.1% peracetic acid had the highest DNA content in comparison with samples from higher acid concentrations and also showed incomplete lipid removal as evidenced by residual yellow lipids in the tissue.

Collagen content in the ECM decreased at higher peracetic acid concentrations, most notably with 5% peracetic acid. The optimal processing condition was determined by ability to best satisfy the two goals of completely removing cellular material while preserving extracellular matrix structure. Ultimately, 3% peracetic acid was determined to give optimal results and was used for subsequent experiments.

SEM images of the decellularized adipose matrix show the fibrillar structure of the ECM with bundles of varying thickness (Fig. 2). The ECM is porous in nature, facilitating cell migration and nutrient diffusion. In vitro experiments with ASCs reveal extensive cell adhesion and spreading on the ECM of the decellularized tissue. Multiple cell-ECM contacts can be seen for each cell by day 7 in culture.

Crosslinking

To control the degradation of the ECM, different chemical crosslinking methods were compared. EDC-crosslinked samples showed greater resistance to enzymatic degradation in comparison to uncrosslinked controls when incubated with collagenase (Fig. 3). Resistance to degradation increased with higher concentrations of the chemical crosslinker. HMDC crosslinking resulted in different degradation profiles depending on the solvent used. For samples reacted in Tween 20, very little degradation was observed with no differences between 1%-5% HMDC concentrations, whereas HMDC in 2-propanol showed greater resistance to enzymatic degradation for 5% HMDC samples compared to 1% HMDC.

In vitro and in vivo analysis

ASCs were alive and proliferating even in the crosslinked conditions. Chemical crosslinkers can be cytotoxic if residual crosslinkers are left in the tissue and the solvents used can also be detrimental to cell survival if incompletely removed. At day 5, cells were predominantly viable and very few dead cells were observed across all three conditions. (See Figure, Supplemental Digital Content 1, which shows results of the live/dead analysis are comparable across control and both crosslinked conditions).

Adipogenic differentiation of ASCs on the adipose-derived biomaterial shows cells adapting a unilocular morphology with adipocytes taking up a single large lipid droplet similar to

their native morphology in adipose tissue. In contrast, ASCs differentiated on traditional 2D tissue culture plates take up multiple small lipid droplets and never develop the characteristic morphology of adipocytes in their natural tissue environment. (See Figure, Supplemental Digital Content 2, which shows the considerable morphological differences between ASCs differentiated in the adipose-derived matrix compared with a tissue culture plate). This suggests that the adipose matrix retains the critical biochemical components that facilitate adipose tissue development, providing the ASCs a more biomimetic environment for adipogenesis.

The in vivo study was carried out with control, 5 mM EDC, and 1% HMDC in Tween 20 crosslinked ECM. After two weeks of implantation, adipose ECM implants were opaque and vascularization could be observed at the surface (Fig. 4). Adipose tissue development was observed at the periphery of the implant. No sign of a severe immune response was evident, but a focal acute inflammatory response was observed at the periphery, extending inwards. The inflammatory reaction was primarily comprised of lymphocytes and neutrophils and the most prominent fibrous capsule formed with the 5 mM EDC crosslinked ECM.

In the long term study, the adipose-derived matrix developed into newly formed adipose tissue at the edges near the scaffold interface with host subcutaneous tissue. Oil Red O staining accentuated the band of adipose tissue forming from the edges of the implant at four weeks (Fig. 5). Additionally, cells in the center of the matrix stained positive for CD31, indicating vascular development, which is the necessary prerequisite for formation of new adipose tissue. A number of cells also stained positive for CD44, a marker for cells of hematopoietic or lymphoid origin involved in the immune response to the biomaterial. By 12 weeks, the adipose tissue development continued in the implant and areas of collagen remodeling were observed by histology (Fig 6).

Discussion

Decellularization of tissues has become increasingly popular as a method to obtain a matrix of proteins and sugars ideally suited to direct the migration of cells into the matrix and provide the structural cues to maintain cell survival.53 A range of applications has been explored for decellularized ECM derived from dermal, cardiovascular, musculoskeletal, hepatic, and gastrointestinal tissues, many of which are already in clinical use and have been shown to facilitate tissue integration and restoration.54

Our studies showed that a decellularized ECM biomaterial can be derived from adipose tissue to obtain a biocompatible scaffold for the repair of soft tissue defects. Crosslinking the decellularized scaffold provided an additional element of control over the degradation properties of the tissue and allows the material to be tailored to the target site of implantation. In vivo implantation in rats revealed good tissue integration with adipose tissue development starting at the edges of the ECM scaffold.

The adipose-derived matrix supported cell migration and infiltration, with a considerable number of host cells at the center of the implant for the uncrosslinked control and 1% HMDC crosslinked matrices. This suggests that despite the acellular nature of the implant, the bioactive properties of the matrix render it conducive to host tissue regeneration. To date, intact adipose-derived ECM has not been studied extensively in vivo for use in soft tissue repair, but results from this study suggest that adipose tissue can be effectively decellularized and stripped of its antigenic components to produce a biocompatible matrix for adipose tissue engineering.

As our understanding of the role of the extracellular matrix in tissue and organ development expands, it is clear that matrix components do not just serve a structural role in tissue, but

also actively participate in the instructional aspect of cell development. Much has recently been elucidated about the role of the various ECM degradation components in influencing cell migration and proliferation, particularly in aiding tissue regeneration.55-57 Studies of adipose tissue ECM proteins have also shown that they facilitate in vivo adipogenesis.37 In view of this instructional role for ECM, we demonstrated that adipose tissue can be successfully processed to remove inflammatory lipids and cells to produce a biomaterial for soft tissue reconstruction.

The components of the adipose-derived scaffold are all naturally occurring ECM proteins and proteoglycans that are highly conserved between different species, such that cells are not exposed to any materials or synthetic polymers that can induce a foreign body response. Host tissue integration is also enhanced since matrix components can be readily degraded by cellsecreted enzymes as tissue remodeling takes place. Mechanisms for matrix turnover are already established in host cells, avoiding any concerns over proper clearance of scaffold materials from the body. These factors contribute to the biocompatibility of ECM-based scaffolds and highlight their utility in regenerative medicine.

Conclusion

Adipose extracellular matrix-based scaffolds offer a promising solution for repair of soft tissue defects whereby they facilitate host tissue regeneration even without the addition of cells. The adipose-derived biomaterial has been shown to be biocompatible, suggesting that allogenic use could potentially provide surgeons with an off-the-shelf product for reconstructive procedures such as craniomaxillofacial surgeries, trauma, and other corrective procedures to restore contour. Consequently, this would avoid many complications encountered with autologous tissue transfer while providing an ideal alternative for patients requiring soft tissue reconstruction.

Supplementary Material

Refer to Web version on PubMed Central for supplementary material.

Acknowledgments

The authors thank the members of the Johns Hopkins Integrated Imaging Center for their technical assistance with scanning electron microscopy and Johns Hopkins Plastic and Reconstructive Surgery for providing tissue samples.

Sources of funding

This work was supported by NIH/NIDCR 5R01DE016887-04 and DOD W81CWH-I1-2-002.

References

1. Wan DC, Lim AT, Longaker MT. Craniofacial autologous fat transfer. J Craniofac Surg. 2009; 20:273–274. [PubMed: 19305242]
2. Cordeiro PG. Breast reconstruction after surgery for breast cancer. N Engl J Med. 2008; 359:1590–1601. [PubMed: 18843123]
3. Rosson GD, Magarakis M, Shridharani SM, et al. A review of the surgical management of breast cancer: plastic reconstructive techniques and timing implications. Ann Surg Oncol. 2010; 17:1890–1900. [PubMed: 20217253]
4. Horl HW, Feller AM, Biemer E. Technique for liposuction fat reimplantation and long -term volume evaluation by magnetic resonance imaging. Ann Plast Surg. 1991; 26:248–258. [PubMed: 2029135]

5. Pulagam SR, Poulton T, Mamounas EP. Long-term clinical and radiologic results with autologous fat transplantation for breast augmentation: case reports and review of the literature. Breast J. 2006; 12:63–65. [PubMed: 16409589]
6. Alderman AK, Wilkins EG, Kim HM, Lowery JC. Complications in postmastectomy breast reconstruction: two-year results of the Michigan Breast Reconstruction Outcome Study. Plast Reconstr Surg. 2002; 109:2265–2274. [PubMed: 12045548]
7. Kroll SS. Fat necrosis in free transverse rectus abdominis myocutaneous and deep inferior epigastric perforator flaps. Plast Reconstr Surg. 2000; 106:576–583. [PubMed: 10987463]
8. Atisha D, Alderman AK. A systematic review of abdominal wall function following abdominal flaps for postmastectomy breast reconstruction. Ann Plast Surg. 2009; 63:222–230. [PubMed: 19593108]
9. Forthomme B, Heymans O, Jacquemin D, et al. Shoulder function after latissimus dorsi transfer in breast reconstruction. Clin Physiol Funct Imaging. 2010; 30:6. [PubMed: 19744087]
10. Spear SL, Hess CL, Elmaraghy MW. Evaluation of abdominal sensibility after TRAM flap breast reconstruction. Plast Reconstr Surg. 2000; 106:1300–1304. [PubMed: 11083559]
11. Rosson GD, Williams CG, Fishman EK, Singh NK. 3D CT angiography of abdominal wall vascular perforators to plan DIEAP flaps. Microsurgery. 2007; 27:641–646. [PubMed: 17941105]
12. Katz RD, Manahan MA, Rad AN, Flores JI, Singh NK, Rosson GD. Classification schema for anatomic variations of the inferior epigastric vasculature evaluated by abdominal CT angiograms for breast reconstruction. Microsurgery. 2010; 30:9.
13. Massey MF, Spiegel AJ, Levine JL, et al. Perforator flaps: recent experience, current trends, and future directions based on 3974 microsurgical breast reconstructions. Plast Reconstr Surg. 2009; 124:737–751. [PubMed: 19730293]
14. Rad AN, Flores JI, Prucz RB, Stapleton SM, Rosson GD. Clinical experience with the lateral septocutaneous superior gluteal artery perforator flap for autologous breast reconstruction. Microsurgery. 2010; 30:339–347. [PubMed: 20073034]
15. Allen RJ, Treece P. Deep inferior epigastric perforator flap for breast reconstruction. Ann Plast Surg. 1994; 32:32–38. [PubMed: 8141534]
16. Alhadlaq A, Tang M, Mao JJ. Engineered adipose tissue from human mesenchymal stem cells maintains predefined shape and dimension: implications in soft tissue augmentation and reconstruction. Tissue Eng. 2005; 11:556–566. [PubMed: 15869434]
17. Hillel AT, Varghese S, Petsche J, Shamblott MJ, Elisseeff JH. Embryonic germ cells are capable of adipogenic differentiation in vitro and in vivo. Tissue Eng Part A. 2009; 15:479–486. [PubMed: 18673089]
18. Shanti RM, Janjanin S, Li WJ, et al. In vitro adipose tissue engineering using an electrospun nanofibrous scaffold. Ann Plast Surg. 2008; 61:566–571. [PubMed: 18948788]
19. Cho SW, Kim SS, Rhie JW, Cho HM, Choi CY, Kim BS. Engineering of volume-stable adipose tissues. Biomaterials. 2005; 26:3577–3585. [PubMed: 15621248]
20. Fischbach C, Seufert J, Staiger H, et al. Three-dimensional in vitro model of adipogenesis: comparison of culture conditions. Tissue Eng. 2004; 10:215–229. [PubMed: 15009947]
21. Choi YS, Park SN, Suh H. Adipose tissue engineering using mesenchymal stem cells attached to injectable PLGA spheres. Biomaterials. 2005; 26:5855–5863. [PubMed: 15949551]
22. Neubauer M, Hacker M, Bauer-Kreisel P, et al. Adipose tissue engineering based on mesenchymal stem cells and basic fibroblast growth factor in vitro. Tissue Eng. 2005; 11:1840–1851. [PubMed: 16411830]
23. Morgan SM, Ainsworth BJ, Kanczler JM, Babister JC, Chaudhuri JB, Oreffo RO. Formation of a human-derived fat tissue layer in P(DL)LGA hollow fibre scaffolds for adipocyte tissue engineering. Biomaterials. 2009; 30:1910–1917. [PubMed: 19135718]
24. Chung HJ, Park TG. Injectable cellular aggregates prepared from biodegradable porous microspheres for adipose tissue engineering. Tissue Eng Part A. 2009; 15:1391–1400. [PubMed: 19327016]
25. Patrick CW Jr, Zheng B, Johnston C, Reece GP. Long-term implantation of preadipocyte-seeded PLGA scaffolds. Tissue Eng. 2002; 8:283–293. [PubMed: 12031117]

26. von Heimburg D, Kuberka M, Rendchen R, Hemmrich K, Rau G, Pallua N. Preadipocyte-loaded collagen scaffolds with enlarged pore size for improved soft tissue engineering. Int J Artif Organs. 2003; 26:1064–1076. [PubMed: 14738190]
27. Hiraoka Y, Yamashiro H, Yasuda K, Kimura Y, Inamoto T, Tabata Y. In situ regeneration of adipose tissue in rat fat pad by combining a collagen scaffold with gelatin microspheres containing basic fibroblast growth factor. Tissue Eng. 2006; 12:1475–1487. [PubMed: 16846345]
28. Hemmrich K, von Heimburg D, Rendchen R, Di Bartolo C, Milella E, Pallua N. Implantation of preadipocyte-loaded hyaluronic acid-based scaffolds into nude mice to evaluate potential for soft tissue engineering. Biomaterials. 2005; 26:7025–7037. [PubMed: 15964623]
29. Hemmrich K, Van de Sijpe K, Rhodes NP, et al. Autologous in vivo adipose tissue engineering in hyaluronan-based gels--a pilot study. J Surg Res. 2008; 144:82–88. [PubMed: 17574595]
30. Kimura Y, Ozeki M, Inamoto T, Tabata Y. Adipose tissue engineering based on human preadipocytes combined with gelatin microspheres containing basic fibroblast growth factor. Biomaterials. 2003; 24:2513–2521. [PubMed: 12695078]
31. Mauney JR, Nguyen T, Gillen K, Kirker-Head C, Gimble JM, Kaplan DL. Engineering adipose-like tissue in vitro and in vivo utilizing human bone marrow and adipose-derived mesenchymal stem cells with silk fibroin 3D scaffolds. Biomaterials. 2007; 28:5280–5290. [PubMed: 17765303]
32. Jing W, Lin Y, Wu L, et al. Ectopic adipogenesis of preconditioned adipose-derived stromal cells in an alginate system. Cell Tissue Res. 2007; 330:567–572. [PubMed: 17922143]
33. Torio-Padron N, Baerlecken N, Momeni A, Stark GB, Borges J. Engineering of adipose tissue by injection of human preadipocytes in fibrin. Aesthetic Plast Surg. 2007; 31:285–293. [PubMed: 17380359]
34. Kawaguchi N, Toriyama K, Nicodemou-Lena E, Inou K, Torii S, Kitagawa Y. De novo adipogenesis in mice at the site of injection of basement membrane and basic fibroblast growth factor. Proc Natl Acad Sci U S A. 1998; 95:1062–1066. [PubMed: 9448285]
35. Kimura Y, Ozeki M, Inamoto T, Tabata Y. Time course of de novo adipogenesis in matrigel by gelatin microspheres incorporating basic fibroblast growth factor. Tissue Eng. 2002; 8:603–613. [PubMed: 12202000]
36. Stillaert F, Findlay M, Palmer J, et al. Host rather than graft origin of Matrigel-induced adipose tissue in the murine tissue-engineering chamber. Tissue Eng. 2007; 13:2291–2300. [PubMed: 17638518]
37. Uriel S, Huang JJ, Moya ML, et al. The role of adipose protein derived hydrogels in adipogenesis. Biomaterials. 2008; 29:3712–3719. [PubMed: 18571717]
38. Choi JS, Yang HJ, Kim BS, et al. Human extracellular matrix (ECM) powders for injectable cell delivery and adipose tissue engineering. J Control Release. 2009; 139:2–7. [PubMed: 19481576]
39. Vermette M, Trottier V, Menard V, Saint-Pierre L, Roy A, Fradette J. Production of a new tissue-engineered adipose substitute from human adipose-derived stromal cells. Biomaterials. 2007; 28:2850–2860. [PubMed: 17374391]
40. Cheng MH, Uriel S, Moya ML, et al. Dermis -derived hydrogels support adipogenesis in vivo. J Biomed Mater Res A. 2010; 92:852–858. [PubMed: 19280638]
41. Abberton KM, Bortolotto SK, Woods AA, et al. Myogel, a novel, basement membrane -rich, extracellular matrix derived from skeletal muscle, is highly adipogenic in vivo and in vitro. Cells Tissues Organs. 2008; 188:347–358. [PubMed: 18354248]
42. Flynn L, Semple JL, Woodhouse KA. Decellularized placental matrices for adipose tissue engineering. J Biomed Mater Res A. 2006; 79:359–369. [PubMed: 16883587]
43. Flynn L, Prestwich GD, Semple JL, Woodhouse KA. Adipose tissue engineering in vivo with adipose-derived stem cells on naturally derived scaffolds. J Biomed Mater Res A. 2009; 89:929–941. [PubMed: 18465826]
44. Brown BN, Freund JM, Han L, et al. Comparison of three methods for the derivation of a biologic scaffold composed of adipose tissue extracellular matrix. Tissue Eng Part C Methods. 2011; 17:411–421. [PubMed: 21043998]
45. Choi JH, Gimble JM, Lee K, et al. Adipose tissue engineering for soft tissue regeneration. Tissue Eng Part B Rev. 2010; 16:413–426. [PubMed: 20166810]

46. Bauer-Kreisel P, Goepferich A, Blunk T. Cell-delivery therapeutics for adipose tissue regeneration. Adv Drug Deliv Rev. 2010; 62:798–813. [PubMed: 20394786]

47. Kim YJ, Sah RL, Doong JY, Grodzinsky AJ. Fluorometric assay of DNA in cartilage explants using Hoechst 33258. Anal Biochem. 1988; 174:168–176. [PubMed: 2464289]

48. Woessner JF Jr. The determination of hydroxyproline in tissue and protein samples containing small proportions of this imino acid. Arch Biochem Biophys. 1961; 93:440–447. [PubMed: 13786180]

49. Olde Damink LH, Dijkstra PJ, van Luyn MJ, van Wachem PB, Nieuwenhuis P, Feijen J. Cross-linking of dermal sheep collagen using a water-soluble carbodiimide. Biomaterials. 1996; 17:765–773. [PubMed: 8730960]

50. Naimark WA, Pereira CA, Tsang K, Lee JM. HMDC cross-linking of bovine pericardial tissue - a potential role of the solvent environment in the design of bioprosthetic materials. Journal of Materials Science-Materials in Medicine. 1995; 6:235–241.

51. Olde Damink LH, Dijkstra PJ, Vanluyn MJA, Vanwachem PB, Nieuwenhuis P, Feijen J. Cross-linking of dermal sheep collagen using hexamethylene diisocyanate. Journal of Materials Science-Materials in Medicine. 1995; 6:429–434.

52. Rault I, Frei V, Herbage D, AbdulMalak N, Huc A. Evaluation of different chemical methods for cross-linking collagen gel, films and sponges. Journal of Materials Science-Materials in Medicine. 1996; 7:215–221.

53. Badylak SF, Freytes DO, Gilbert TW. Extracellular matrix as a biological scaffold material: Structure and function. Acta Biomater. 2009; 5:1–13. [PubMed: 18938117]

54. Gilbert TW, Sellaro TL, Badylak SF. Decellularization of tissues and organs. Biomaterials. 2006; 27:3675–3683. [PubMed: 16519932]

55. Reing JE, Zhang L, Myers-Irvin J, et al. Degradation products of extracellular matrix affect cell migration and proliferation. Tissue Eng Part A. 2009; 15:605–614. [PubMed: 18652541]

56. Brennan EP, Tang XH, Stewart-Akers AM, Gudas LJ, Badylak SF. Chemoattractant activity of degradation products of fetal and adult skin extracellular matrix for keratinocyte progenitor cells. J Tissue Eng Regen Med. 2008; 2:491–498. [PubMed: 18956412]

57. Tottey S, Corselli M, Jeffries EM, Londono R, Peault B, Badylak SF. Extracellular matrix degradation products and low oxygen conditions enhance the regenerative potential of perivascular stem cells. Tissue Eng Part A. 2010

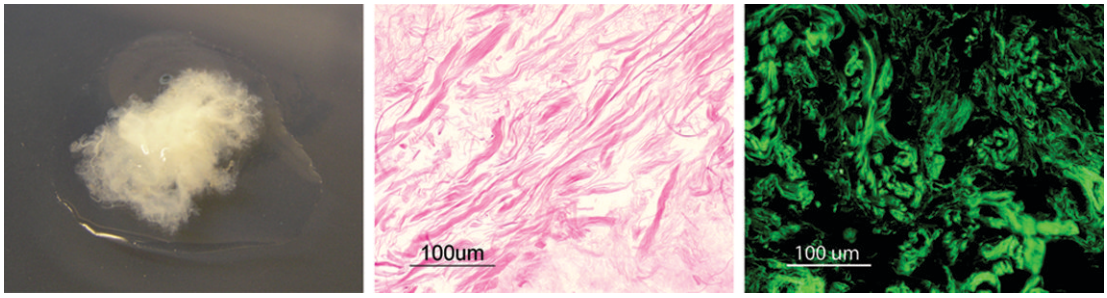

Figure 1.
Processed adipose tissue matrix (left) and histological image of decellularized adipose tissue showing no remnants of cellular components (center). Immunostaining for type I collagen confirms it as the predominant component of adipose extracellular matrix (right).

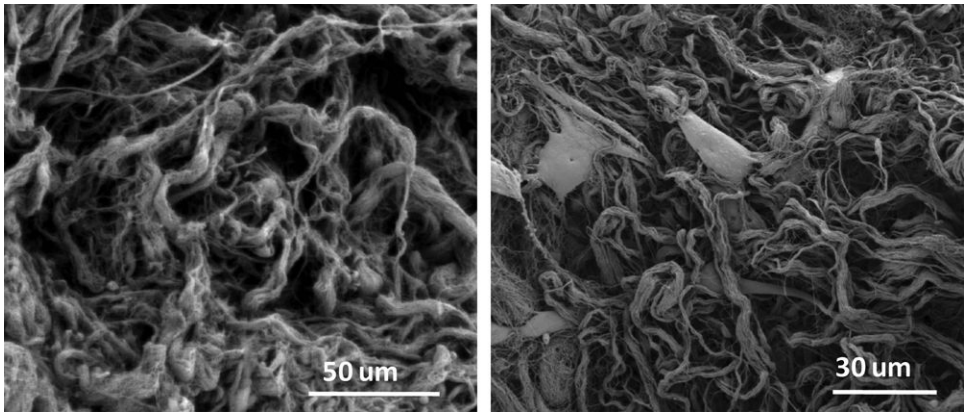

Figure 2.
Scanning electron microscopy images of processed adipose ECM without cells (left) and 48 hours after seeding with cells (right).

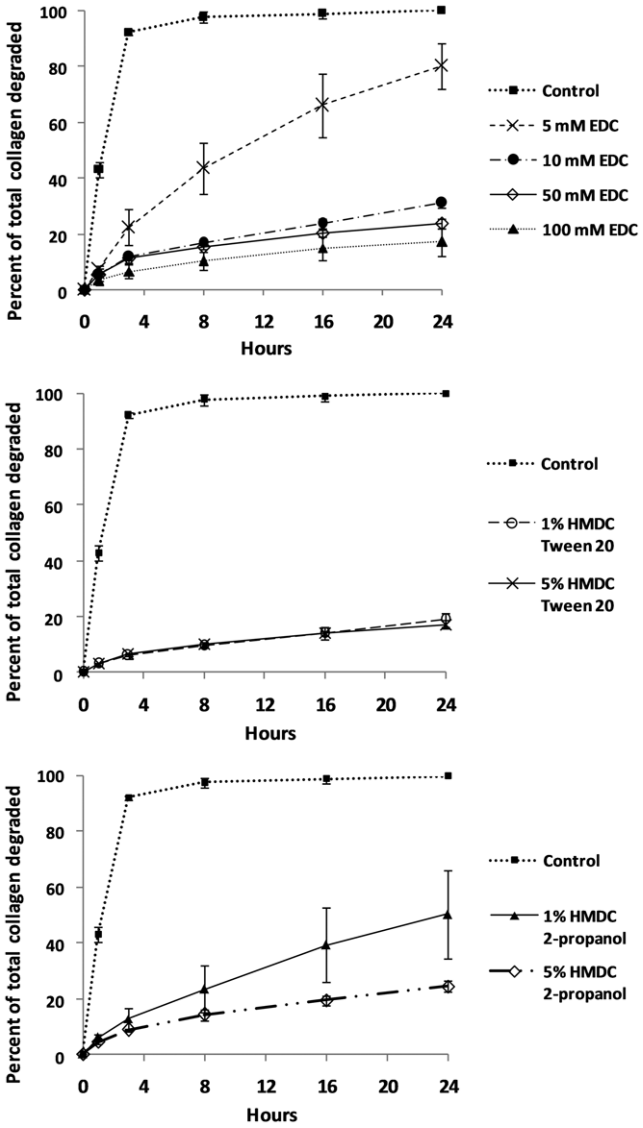

Figure 3.

Crosslinked matrices show increased resistance to enzymatic degradation. Percent of total collagen degraded over 24 hours when incubated with collagenase for uncrosslinked control tissue and matrices crosslinked with 5-100 mM EDC (above), 1% and 5% HMDC in Tween 20 (center), 1% and 5% HMDC in 2-propanol (below). Error bars denote standard deviation.

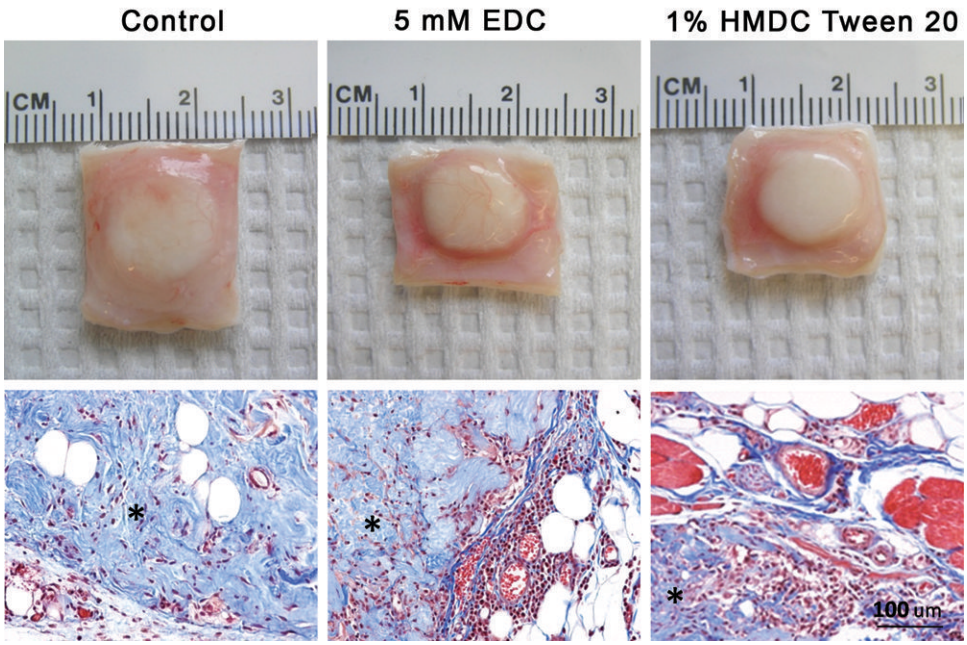

Figure 4.

Gross (above) and histological images (below) of adipose matrix from the in vivo rat study for uncrosslinked control (left), 5 mM EDC crosslinked (center), and 1% HMDC crosslinked ECM (right). Specimens are stained with Masson's trichrome and the adiposederived matrix is denoted by an asterisk.

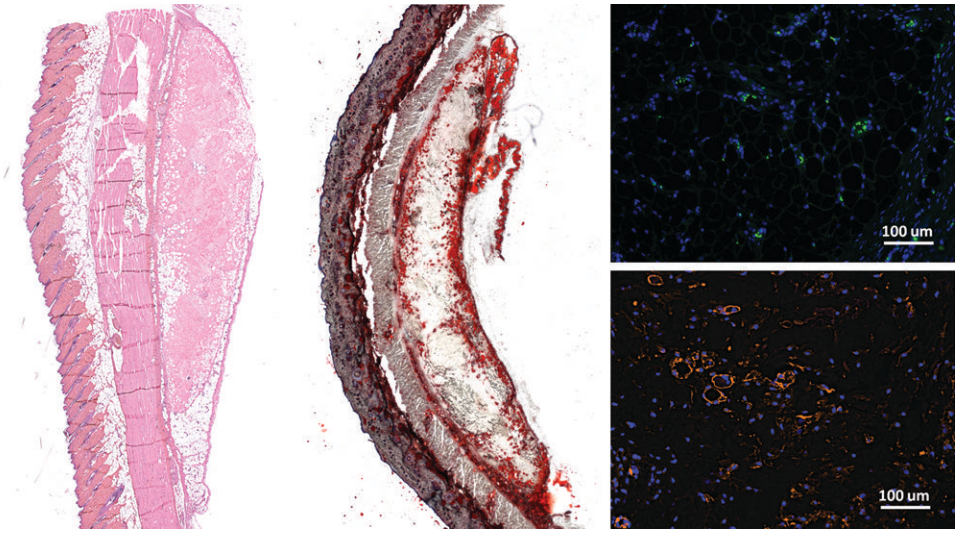

Figure 5.
Histology of adipose ECM implants after four weeks in Sprague Dawley rats stained with hematoxylin and eosin (left), Oil red O for lipids (center), CD31 (above, right), and CD44 (below, right).

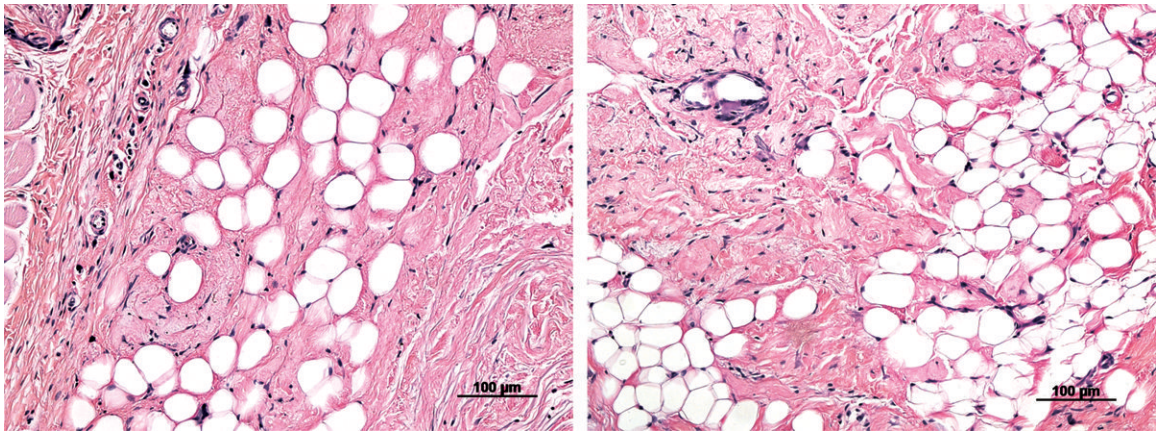

Figure 6.
At 12 weeks in the subcutaneous rat study, adipose matrix implants show substantial areas of adipose tissue development and collagen remodeling by host cells.